



SIMULATION OF THE TEMPERATURE AND GRAIN SIZE DEPENDENT UNIAXIAL COMPRESSIVE STRENGTH USING 3D WING CRACK MODEL

Kari Kolari¹

¹VTT Technical Research Centre of Finland, Espoo, Finland

ABSTRACT

A number of measurements of uniaxial compressive strength of sea ice and fresh water ice have shown that the strength increases with decreasing temperature. Also the kinetic ice-ice friction increases with decreasing temperature. During compression number of micro-cracks initiate and propagate. Frictional sliding of these cracks play significant role in the deformation process; increase of the strength is a result from the increased friction.

In this paper the effect of temperature dependent kinetic friction and the effect of grain diameter on the compressive strength are studied using the new 3D wing crack model. The two dimensional kinematic sliding crack model has been extended into three dimensions to describe the inelastic deformation mechanism. Interaction of cracks and the inhomogeneity of material are considered in the approach. The model has been implemented into finite element software as a user subroutine.

The numerical simulations revealed good results compared to experimental results found in the literature. The proposed approach was found to be capable to simulate the increase of the compressive strength with decreasing temperature. In addition the model was found to be capable to simulate the increasing trend of strength as a function of decreasing grain diameter.

INTRODUCTION

The modelling of brittle failure under compression is one of the greatest challenges in material failure analysis of rock, concrete, ceramics and natural ice. Formation, growth and interaction of (micro) cracks due to the material inhomogeneities and external force is considered to be the mechanism of brittle failure in uniaxial compression (Nemat-Nasser and Horii, 1984). One of the mechanisms proposed for modelling of axial splitting is the sliding or the 'wing crack' model. Frictional sliding of internal cracks play significant role in the model.

The compressive strength of granular ice is known to be a function of temperature, grain size, strain rate and porosity. At brittle regime temperature and grain size play a significant role; as the grain size or temperature increases the strength decreases (Cole, 1987; Schulson, 1990). The compressive strength increases with decreasing temperature by $\sim 0.3 \text{ MPa}^\circ\text{C}^{-1}$ (Schulson and Duval, 2009, p. 245). The strength depends on the grain size through the relationship $\sim d^{-1/2}$, where d is the grain diameter (Schulson, 1990).

Recent studies have shown that the kinetic ice-ice friction μ is strongly dependent on temperature and sliding velocity (Makkonen and Tikanmäki, 2014; Schulson and Fortt, 2012). At the velocity range of $10^{-4} \dots 10^{-1} \text{ m/s}$ the coefficient of friction decreases with the increasing rate. Similarly the coefficient of friction increases when temperature decreases (Cole, 1987;

Schulson, 1990). At the sliding velocity of 10^{-4} m/s the coefficient increases from $\mu = 0.3$ at -3 °C to $\mu = 0.75$ at -40 °C.

OBJECTIVES AND SCOPE

The objective is to study if 3D-wing crack model can be applied to model compressive strength of ice and especially the dependence of grain size and temperature. Only granular ice is considered in this study.

WING CRACK MODEL

As stated above the wing crack model has been proposed to explain the failure of various brittle materials under uniaxial compression (Ashby and Hallam, 1986; Brace and Bombolakis, 1963; Fairhurst and Cook, 1966; Renshaw and Schulson, 2001). As illustrated in Figure 1a the failure begins when a primary crack undergoes frictional sliding, creating secondary cracks at the tips of the primary crack. The macroscopic failure occurs when series of cracks extend and finally link together and split the material. It has been shown, that the size of the primary crack is directly related to the grain size (Cole, 1987; Picu and Gupta, 1995); therefore the wing crack model can be linked both to the grain size and to the temperature dependent friction of ice as proposed by Schulson (1990).

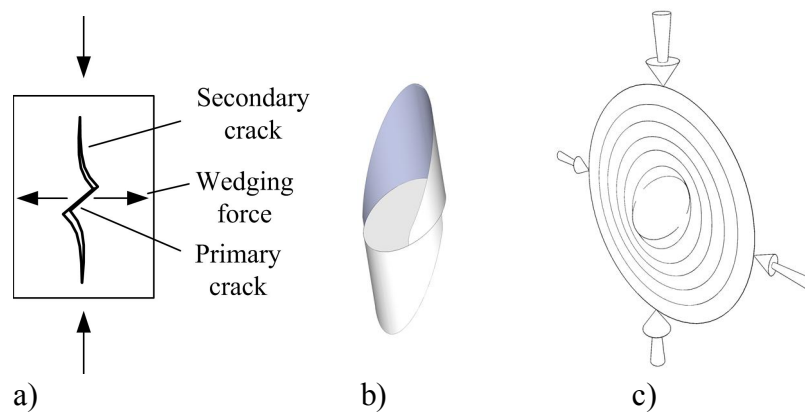


Figure. 1. Sliding cracks. (a) 2D crack; (b) Wrapping of single 3D crack under uniaxial compression; (c) 3D crack under biaxial compression.

Wing Crack in 3D

The wing-crack model has been widely studied in 2D. The models fit well to the test results (e.g. Nemat-Nasser and Horii, 1982). The mechanism in 3D is somewhat different to that of 2D; under uniaxial loading of single, inclined primary crack the secondary crack wraps (curves) as illustrated in Fig. 1b (Adams and Sines, 1978; Cannon et al., 1990; Dyskin et al., 1994). In the uniaxial compression tests of polyester resin (Dyskin et al., 1994) wings were found to grow in stable manner until the length of the wrapped wing was 1.0-1.5 times the diameter of the primary crack. Under further loading wings did not grow.

3D WING-CRACK MODEL

Consider compressed medium embedded with several inclined primary cracks. As stated before, in three dimensions single secondary crack has been shown to wrap around the primary crack. But under biaxial loading the wrapping is prevented and the global failure mode is splitting and formation of slabs, where the normal to the slabs is parallel to the no-loaded direction as show experiments of Weiss and Schulson (1995) and Sahouryeh et al. (1998; 2002) and illustrated in Fig.1.

The interaction of closely spaced penny shaped cracks in 3D medium has been found to be important; the tests and observations of Dyskin et al. (2003) imply that interaction of multitude cracks can produce substantial crack growth and finally cause splitting along vertical columns.

Based on the observations above the model is based on the following assumptions: a) because of the interaction instead of wrapping the secondary crack is assumed to grow in plane; b) both the primary and the secondary cracks can be described as penny shaped cracks (Fig. 2); c) the interaction of cracks is important and has to be is modelled.

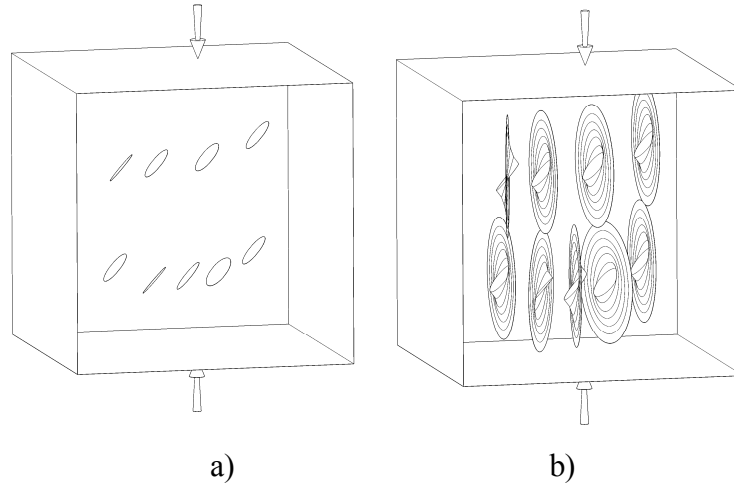


Figure. 2. Illustration of the 3D-Wing crack model; (a) primary cracks and (b) secondary cracks.

Kinematic Model

Only the main features of the proposed model are presented in this paper. The model has been described in detail by Kolari (2013). Isometric and section views of a 3D Penny shaped cracks are illustrated in Figure 3a and 3b. The diameters of the primary and secondary cracks are a_0 and L respectively. The unit normal vector \mathbf{N} of the primary crack defines the orientation of the primary crack while the vector \mathbf{n} represents the unit normal of the crack tip.

Consider representative crack BB' shown in Figure 3c subjected to concentrated force pair denoted \mathbf{R} . Forces represent the effect of the sliding primary crack AA'. The magnitude R of the splitting force \mathbf{R} is defined as follows:

$$R = \pi a_0^2 \tau^* \quad (1)$$

where the effective shear τ^* is assumed to be evenly distributed over the primary crack. The effective shear defined as

$$\tau^* = \tau^N + \mu \sigma^N - \tau^c \quad (2)$$

where μ is friction coefficient and τ^c is the cohesion. The normal traction σ^N and shear traction τ^N are defined as

$$\begin{aligned} \sigma^N &= \mathbf{N} \cdot \boldsymbol{\sigma} \cdot \mathbf{N} \\ \tau^N &= \sqrt{\mathbf{N} \cdot \boldsymbol{\sigma} \cdot \boldsymbol{\sigma} \cdot \mathbf{N} - (\sigma^N)^2} \end{aligned} \quad (3)$$

where $\boldsymbol{\sigma}$ is stress tensor.

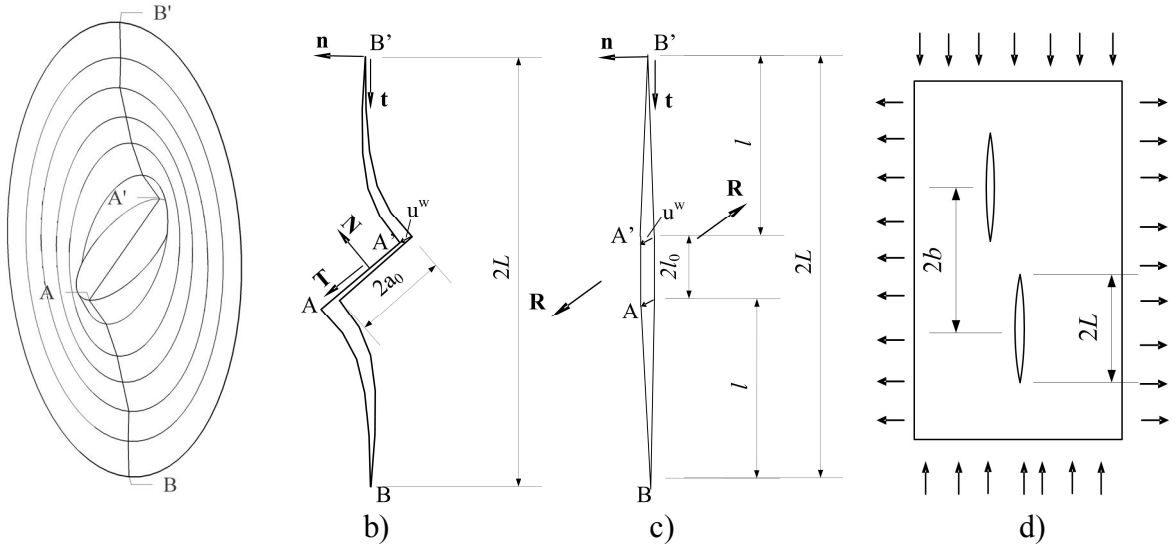


Figure. 3. 3D-Wing crack and its section views: (a) Isometric view; (b) section view along the line B-B'; (c) the representative straight crack model for crack propagation calculations; (d) average spacing of cracks. Notations: \mathbf{N} and \mathbf{T} are unit normal vectors along the direction of normal and shear tractions on the primary crack; \mathbf{n} and \mathbf{t} are unit normal vectors along the direction of normal and shear tractions at the tip of the secondary crack; \mathbf{R} is the crack opening traction.

Stress-strain relation

The Gibbs energy density ψ for representative volume of V_0 is given as

$$\begin{aligned} \psi &= \frac{1}{2E} \left[(1 + \nu) \sigma_{kl} \sigma_{kl} - \nu (\sigma_{kk})^2 \right] \\ &+ \frac{1 - \nu^2}{E V_0} \sum_{k=1}^p 2 \int_0^L \int_0^{2\pi} \left[(K_I)^2 + (K_{II})^2 + (K_{III})^2 \right] d\theta dL \end{aligned} \quad (4)$$

where p is the number of cracks in V_0 , ν is Poisson's ratio, E is Young's modulus. The stress intensity factors K_I , K_{II} and K_{III} are functions of the splitting force \mathbf{R} and stress

tensor σ . The factors are explicitly given by Kolari (2013). The interaction of cracks depends e.g. on the orientation and spacing of cracks which is not known. To take account the interaction of cracks the stress intensity factors have been multiplied by crack interaction function $g(L/b)$. The function has chosen such that $g(L/b) \rightarrow \infty$ when $L = b$, where b is the spacing of cracks:

$$g(L/b) = \left(1 - \frac{L^2}{b^2}\right)^{-1/2} \quad (5)$$

The strain-stress relation is obtained from (4) as follows

$$\varepsilon_{ij} = \frac{\partial \psi}{\partial \sigma_{ij}} \quad (6)$$

Crack evolution

The crack growth is based on linear elastic fracture mechanics. Similar to the 2D model the crack length L is obtained from the following criterion:

$$f = K_I - K_{IC} = 0 \quad (7)$$

where K_I is the stress intensity factor for mode I and K_{IC} is the fracture toughness. The growth criterion of Eq. (7) is applicable only when crack growth is stable i.e. $\partial K_I / \partial L < 0$. If the interaction of cracks was neglected the growth of wing crack under compression would be stable. Due to the crack interaction function of Eq.(5) the growth becomes unstable when $L / b \approx 0.8$. Therefore, when $K_I > K_{IC}$ and $\partial K_I / \partial L > 0$ a new growth criteria has to be introduced. It is simply assumed that in the unstable range the growth rate is constant: $dL / dt = v_c$, where dt is the time increment and v_c is the crack velocity. Then the crack length increment is written as follows:

$$dL = v_c dt \quad (8)$$

In 1993 Xie and Farmer observed that the grain size crack velocity is of order 400 m/s (cited in Dempsey, 2000). In this paper it is simply assumed that v_c in Eq. (8) equals 400 m/s.

Crack nucleation and primary crack diameter

The initiation and growth of the primary crack is out of the scope of this work. Therefore simplified approach is applied in this paper. The primary crack is assumed to initiate and grow into the direction of the maximum shear stress. The critical initiation stress τ_c for columnar ice is as follows (Picu and Gupta, 1995):

$$\tau_c = \tau_b + \sqrt{\frac{3}{2\pi}} K_{IC} d^{-1/2} \quad (9)$$

where d is the grain diameter and τ_b is a threshold boundary sliding resistance depending on the temperature and rate. At -10 °C and strain rate of $10^{-3} 1/s$ the threshold has the value of

0.18 MPa (Picu and Gupta, 1995). When maximum shear stress exceeds the value of the critical stress of Eq. (9) primary crack of radius $a_0 = 0.65 \cdot d / 2$ will be born into the direction defined by the principal shear.

BRITTLE COMPRESSIVE STRENGTH OF GRANULAR ICE

Grain size

According to the experimental studies of Cole (1986) “strength generally decreased with increasing grain-size but the effect was variable.” Schulson (1990) observed the same trend and proposed the following strength-grain function

$$\sigma_c = \sigma_0 + k_c d^{-p} \quad (10)$$

where σ_c is compressive strength, σ_0 and k_c are material constants and $p=1/2$. Figure 4 shows experimental results and a linear trend line fitted to the results.

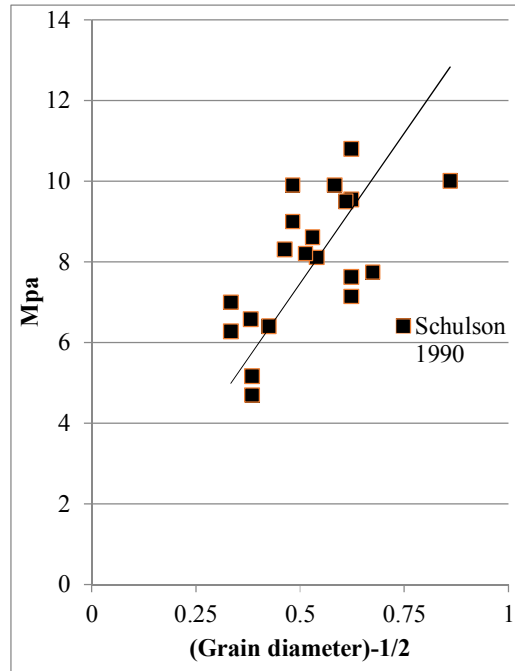


Figure. 4. Compressive strength of polycrystalline granular freshwater ice as a function of grain size^{-1/2} (mm^{-1/2}) at -10 °C with strain rate of 10⁻³ s⁻¹. Tests by Schulson (1990), data obtained from Nixon (1996); The trend line is drawn such that $\sigma_0 = 0$ in. Eq. (10).

According experiments of Cole (1986) nucleated cracks are proportional to grain size. The ratio of crack size to grain diameter was found to be 0.65. Also the density of cracks increases with increasing grain diameter (ibid.). Sanderson (1988) suggested that for grains larger than 5 mm it is reasonable to assume the formation of one crack per grain. According to the measurements of Schulson et al. (1990) crack spacing was 4.7 mm – 8 mm for granular ice of 3 mm and 9 mm grain size. The distribution was measured at the peak load.

Temperature and kinetic friction

Sanderson (1988, p. 94) assumed that the friction across crack is very temperature dependent. He suggested that the kinetic friction coefficient lies in the range of 0-0.3. As illustrated in

Figure 5 it has been shown later that the friction range is wider than assumed by Sandersson: the range is 0-0.8 (Kennedy et al., 2000; Schulson, 1990). Compressive strength and kinetic friction of ice is known to increase with decreasing temperature (Arakawa and Maeno, 1997; Schulson, 1990) as illustrated in Figure 5. Sanderson (1988), Cannon et al. (1990) and Schulson (1990) link the temperature dependent friction and the temperature dependent compressive strength to the wing crack model; the strength change can be considered to be caused by the temperature dependent friction.

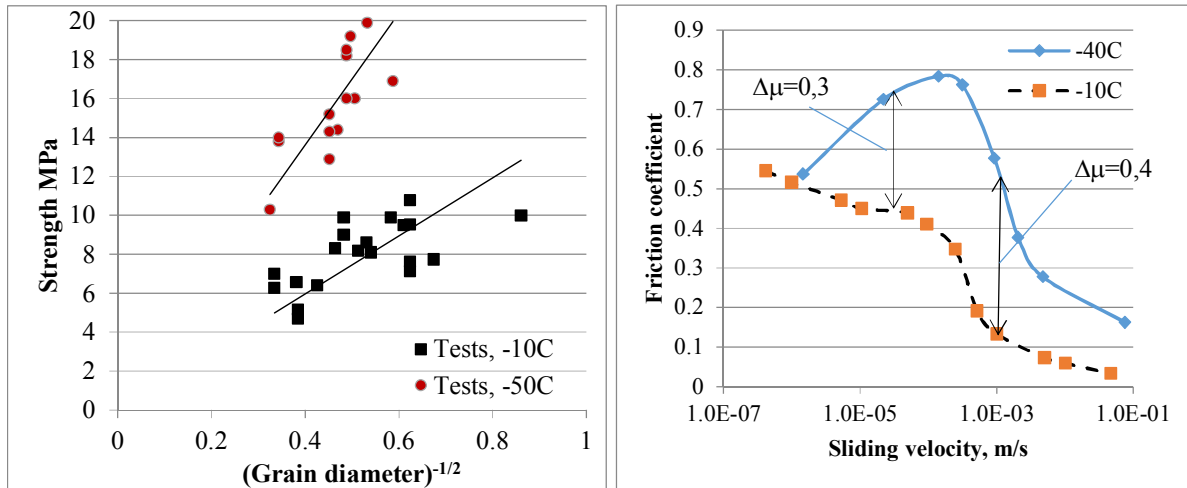


Figure. 5. Left: Compressive strength of polycrystalline granular freshwater ice as a function of temperature and grain size when strain rate equals 10^{-3} s^{-1} (Tests by Schulson (1990), data from Nixon (1996)). Right: Kinetic friction vs temperature and sliding velocity (redrawn from Schulson, 1990).

NUMERICAL SIMULATION – STRENGTH, GRAIN SIZE & FRICTION

The objective of the numerical simulation was to study uniaxial compressive strength as a function of grain size and coefficient of kinetic friction. For the sake of simplicity the effect of sliding-velocity was not considered.

FE-Model – Uniaxial Compression Simulation

Abaqus/Explicit FE-software was used in the simulation. The wing crack model proposed by Kolari (2013) was implemented into the software as a user subroutine. The specimen of $10 \times 10 \times 10 \text{ cm}^3$ shown in Figure 6 was modelled using 3D elements of type C3D8R. The number of elements was 125. The specimen was loaded using rigid loading platen such that contact between platen and specimen was frictionless. Vertical displacements of the bottom of the specimen were fixed. Both the top and bottom surfaces were free of lateral constraints. The compression was simulated pushing the platen downwards with constant velocity of 0.3 mm/s.

Material Properties

The spacing of cracks is not well known; Cole (1986) found that spacing is inversely proportional to the grain size, at 1990 Couture found crack spacing to be $\sim 2d$ for columnar ice of 5 mm grain size (Schulson and Duval, 2009, p. 249). In the numerical simulations the spacing of cracks is set to $2a_0$ where $a_0 = 0.65d$.

It is well known that grain size varies in test specimens; cracks are never exactly of the same size. To simulate small deviation in grain size it was assumed that grain size varies log-normally; the standard deviation was set to $0.1 \cdot 2a_0$.

The material parameters used in the simulation were the following:

$$\begin{aligned} E &= 9.0 \text{ GPa} \\ \nu &= 0.3 \\ a_0 &= 0.65d / 2 \text{ (primary crack diameter)} \\ 2b &= 2a_0 \text{ (crack spacing)} \\ \tau^c &= 0.01 \text{ MPa (cohesion)} \\ K_{IC} &= 37 \text{ kPa}\sqrt{\text{m}} \\ \rho &= 917 \text{ kg/m}^3 \end{aligned}$$

where ρ is the density of ice.

Numerical Results

The friction coefficient μ was varied in the range of 0.1-0.9 and the diameter of grains d in the range of 1.0-10.0 mm. The simulated compressive strength vs grain diameter and friction coefficient is shown in Figure 7.

Sandersson (1988) estimated compressive strength using the wing crack model of Ashby and Hallam (1986). He derived the following simplified equation for uniaxial compressive strength:

$$\sigma_c = 7.6 K_{IC} \sqrt{d} \quad (11)$$

where he assumed that $2a_0 = 0.65d$ and $\mu = 0.3$. Sandersson's estimate is plotted in Figure 7.

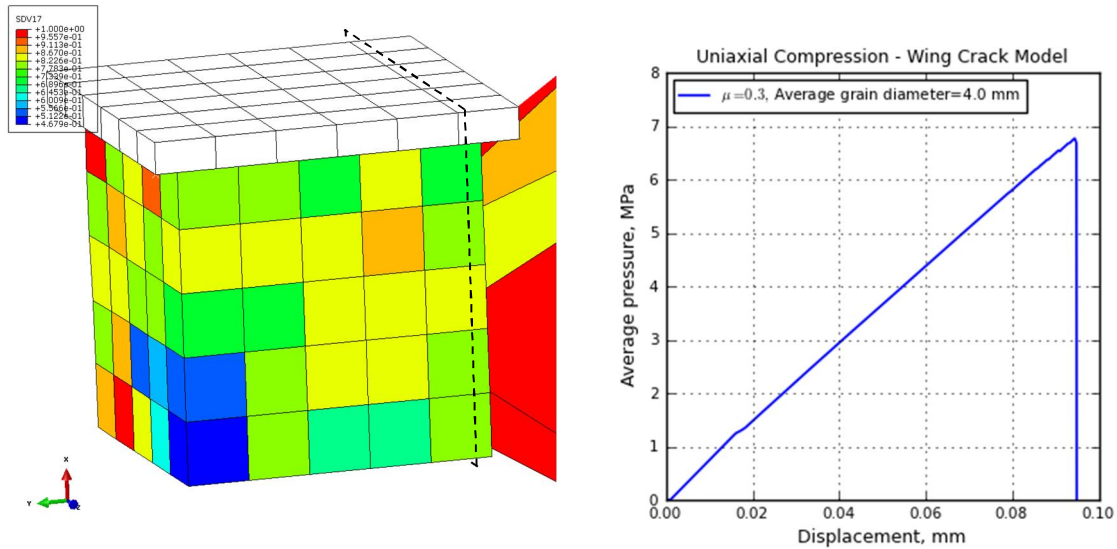


Figure. 6. Contour plot of crack length-spacing ratio (L/b) after peak stress (lhs); Displacement vs average pressure (rhs), when $\mu = 0.3$ and $d = 4.0$ mm. The dashed line represents the view cut plane of Figure 8. Elements distort highly after brittle failure (lhs).

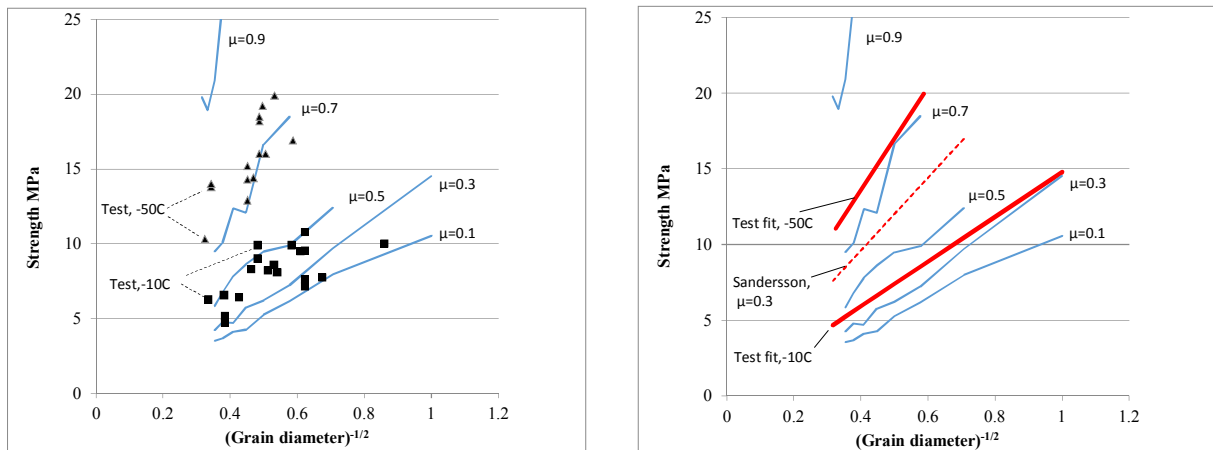


Figure. 7. Simulated results as a function of grain diameter and friction (thin blue lines). Markers represent test results and thick red lines represent fitted test results of Schulson (1990).

Discussion on Numerical Results

Two observations can be made based on the orientations of secondary cracks illustrated in Figure 8: the side view shows that all cracks are almost parallel and normal to the loading while the top view shows that crack normals are not parallel. It means that the failure mode is “*column like splitting*”. If normals were parallel, the failure mode was splitting along vertical planes.

As shown in the load-displacement curve of Figure 6 (rhs), the brittle like failure was successfully simulated with the model; load drops suddenly after peak force.

Numerical simulations showed that the *crack growth was localised*. This uneven distribution of crack growth is illustrated in Figure 6 (lhs). It shows that L/b (crack-length/spacing) ratio is clearly uneven. In numerical simulations the localisation is can be caused e.g. by round of errors but in this case the small deviation introduced in diameter of grains is driving the

localisation. Therefore simulations resemble experimental tests where damage also tends to localise.

In addition to the localised growth of cracks it was noticed that *cracks grew jerky manner*. Therefore the sliding velocity was not constant at all. Typical sliding velocity was rather high and varied, being order of 10^{-5} - 10^{-4} m/s before peak stress. That corresponds to the coefficient of friction of ~ 0.4 at -10 °C and ~ 0.7 at -40 °C (see Figure 5 (rhs)).

As shown in Figure 7 the 3D wing crack model describes reasonable well the relationship between strength and grain diameter. Sandersson's (1988) estimate plotted in the figure is based on the use of friction coefficient of 0.3. His estimate is close to 3D wing crack model simulations with the friction coefficient of 0.6.

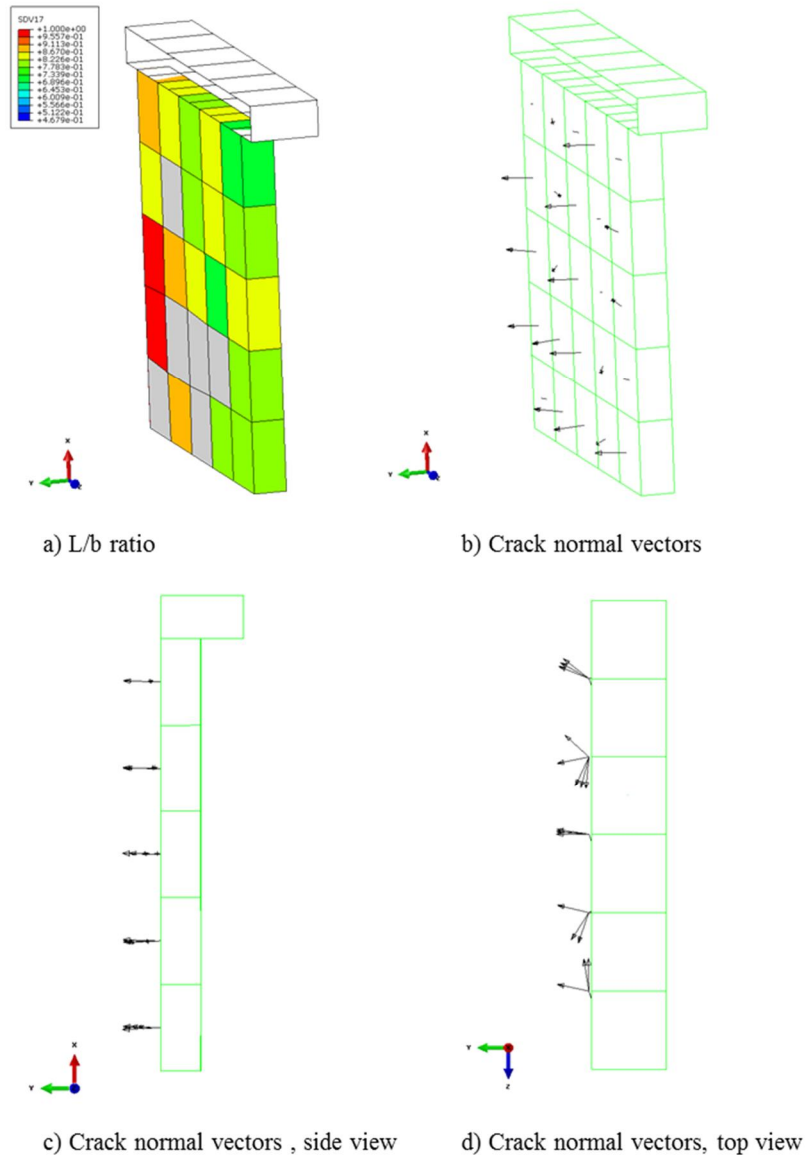


Figure. 8. View cut based on the plane illustrated in Figure 6. a) Crack length spacing ratio L/b ; b-d) the orientation of secondary cracks, when $\mu = 0.3$ and $d = 4.0$ mm. Vectors represent the normal \mathbf{n} of secondary cracks (see Figure 3).

The small deviation in grain size has impact on the results of numerical simulations. Simulated strength – grain size curves appear to be straighter when the coefficient of friction is low (see Figure 7); the scatter increases with increasing friction.

The difference $\Delta\mu$ in friction coefficient between -10°C and -40°C is about 0,4 in the velocity range of $5.0 \cdot 10^{-5} \dots 1.0 \cdot 10^{-3}$ m/s as illustrated in Figure 5 (rhs). If we assume that the coefficient of friction at -10°C is 0.4 and 0.7 at -50°C respectively, numerical simulations fit reasonable well to the experimental results.

CONCLUSIONS

The numerical simulations showed that the 3D-wing crack approach models very well the relation between strength and grain diameter. The increase of compressive strength with decreasing temperature was also successfully simulated based on the temperature dependent friction. The simulated failure mode was column-like splitting. Contrary to the Nixon's (1996) conclusions, on the basis of the results shown in this paper wing crack model could be applied to predict the brittle compressive failure of ice. Further information on the effect of temperature and sliding velocity on kinetic friction is needed for the further improvement of the model.

ACKNOWLEDGEMENT

The author acknowledges Erland M. Schulson and Knut Høyland for the interesting discussions, comments and their hospitality during his stay in NTNU, Norway. The author wish to acknowledge the support from the following projects: SAMCoT (funded by Research Council of Norway and industry partners); ARNOR (funded by Tekes - the Finnish Funding Agency for Technology and Innovation and industry partners); DICE (funded by the Academy of Finland).

REFERENCES

- Adams, M. & Sines, G. 1978. Crack extension from flaws in a brittle material subjected to compression. *Tectonophysics*, Vol. 49, No. 1–2, pp. 97–118. ISSN 0040-1951
- Arakawa, M. & Maeno, N. 1997. Mechanical strength of polycrystalline ice under uniaxial compression. *Cold Regions Science and Technology*, Vol. 26, No. 3, pp. 215–229.
- Ashby, M. F. & Hallam, N. C. 1986. The failure of brittle solids containing small cracks under compressive stress states. *Acta Metallurgica*, Vol. 34, No. 3, pp. 497–510.
- Brace, W. F. & Bombolakis, E. G. 1963. A Note on Brittle Crack Growth in Compression. *J Geophys Res*, Vol. 68, No. 12, pp. 3709–3713. ISSN 0148-0227
- Cannon, N. P., Schulson, E. M., Smith, T. R. & Frost, H. J. 1990. Wing cracks and brittle compressive fracture. *Acta Metallurgica et Materialia*, Vol. 38, No. 10, pp. 1955–1962.
- Cole, D. M. 1986. Effect of grain size on the internal fracturing of polycrystalline ice. CRREL Report No. 86-5. 79 p.
- Cole, D. M. 1987. Strain-rate and grain-size effects in ice. *Journal of Glaciology*, Vol. 33, No. 115, pp. 274–280.
- Dempsey, J. P. 2000. Research trends in ice mechanics. *International Journal of Solids and Structures*, Vol. 37, No. 1-2, pp. 131–153.

Dyskin, A. V., Jewell, R. J., Joer, H., Sahouryeh, E. & Ustinov, K. B. 1994. Experiments on 3-D crack growth in uniaxial compression. *Int J Fract*, Vol. 65, No. 4, pp. R77–R83. ISSN 0376-9429

Fairhurst, C. & Cook, N. G. W. 1966. The phenomenon of rock splitting parallel to the direction of maximum compression in the neighbourhood of a surface. *Proceedings of the 1st International Congress of Rock Mechanics*. Pp. 687–692.

Kennedy, F. E., Schulson, E. M. & Jones, D. E. 2000. The friction of ice on ice at low sliding velocities. *Philosophical Magazine A*, Vol. 80, No. 5, pp. 1093–1110. ISSN 0141-8610

Kolari, Kari. 2013. Simulation of Brittle Failure of Ice. In: Polojärvi, Arttu and Tuhkuri, Jukka (ed.). 22th international conference on port and ocean engineering under arctic conditions, POAC '13. June 9-13, 2013, Espoo, Finland. 9-6-2013. Pp. 1–12. ISSN 2077-7841

Makkonen, L. & Tikanmäki, M. 2014. Modeling the friction of ice. *Cold Regions Science and Technology*, Vol. 102, No. 0, pp. 84–93. ISSN 0165-232X

Nemat-Nasser, S. & Horii, H. 1982. Compression-induced nonplanar crack extension with application to splitting, exfoliation, and rockburst. *Journal of Geophysical Research*, Vol. 87, No. B8, pp. 6805–6821.

Nemat-Nasser, S. & Horii, H. 1984. Rock Failure in Compression. *International Journal of Engineering Science*, Vol. 22, No. 8-10, pp. 999–1011.

Nixon, W. A. 1996. Wing crack models of the brittle compressive failure of ice. *Cold Regions Science and Technology*, Vol. 24, No. 1, pp. 41–55.

Picu, R. C. & Gupta, V. 1995. Observations of crack nucleation in columnar ice due to grain boundary sliding. *Acta Metallurgica et Materialia*, Vol. 43, No. 10, pp. 3791–3797.

Renshaw, C. E. & Schulson, E. M. 2001. Universal behaviour in compressive failure of brittle materials. *Nature*, Vol. 412, No. 6850, pp. 897–900. ISSN 0028-0836

Sahouryeh, E., Dyskin, A. V., & Germanovich, L. N. 1998. A mechanism of 3-D crack growth and splitting in biaxial compression. ECF12. ESIS. Fracture from Defects. Proceedings of the 12th Biennial Conference on Fracture, 14-18 Sept. 1998. Cradley Heath, UK: Eng. Mater. Advisory Services. Vol. vol.2. Pp. 745–750.

Sahouryeh, E., Dyskin, A. V. & Germanovich, L. N. 2002. Crack growth under biaxial compression. *Engineering Fracture Mechanics*, Vol. 69, No. 18, pp. 2187–2198. ISSN 0013-7944

Sanderson, T. J. O. 1988. *Ice Mechanics: Risks to Offshore Structures*. London: Graham and Trotman. 253 p. ISBN 0-86010-785-X

Schulson, E. M. 1990. The brittle compressive fracture of ice. *Acta Metallurgica et Materialia*, Vol. 38, No. 10, pp. 1963–1976.

Schulson, E. M. & Duval, P. 2009. *Creep and Fracture of Ice*. Cambridge University Press. 416 p. ISBN 9780521806206

Schulson, E. M. & Fortt, A. L. 2012. Friction of ice on ice. *Journal of Geophysical Research: Solid Earth*, Vol. 117, No. B12204, pp. 1–18. ISSN 2156-2202

Weiss, J. & Schulson, E. M. 1995. The failure of fresh-water granular ice under multiaxial compressive loading. *Acta Metallurgica et Materialia*, Vol. 43, No. 6, pp. 2303–2315.